Journal of Hazardous Materials 166 (2009) 79–87

Contents lists available at ScienceDirect

Journal of Hazardous Materials

journal homepage: www.elsevier.com/locate/jhazmat

Characterizing the discoloration of methylene blue in Fe^0/H_2O systems

C. Noubactep*

Angewandte Geologie, Universität Göttingen, Goldschmidtstraße 3, D-37077 Göttingen, Germany

ARTICLE INFO

Article history:
Received 13 July 2008
Received in revised form 12 October 2008
Accepted 3 November 2008
Available online 7 November 2008

Keywords:
Adsorption
Co-precipitation
Iron corrosion
Methylene blue
Zerovalent iron

ABSTRACT

Methylene blue (MB) was used as a model molecule to characterize the aqueous reactivity of metallic iron in Fe^0/H_2O systems. Likely discoloration mechanisms under used experimental conditions are: (i) adsorption onto Fe^0 and Fe^0 corrosion products (CP), (ii) co-precipitation with in situ generated iron CP, (iii) reduction to colorless leukomethylene blue (LMB). MB mineralization (oxidation to CO_2) is not expected. The kinetics of MB discoloration by Fe^0, Fe_2O_3, Fe_3O_4, MnO_2, and granular activated carbon were investigated in assay tubes under mechanically non-disturbed conditions. The evolution of MB discoloration was monitored spectrophotometrically. The effect of availability of CP, Fe^0 source, shaking rate, initial pH value, and chemical properties of the solution were studied. The results present evidence supporting co-precipitation of MB with in situ generated iron CP as main discoloration mechanism. Under high shaking intensities (>150 min^{-1}), increased CP generation yields a brownish solution which disturbed MB determination, showing that a too high shear stress induced the suspension of in situ generated corrosion products. The present study clearly demonstrates that comparing results from various sources is difficult even when the results are achieved under seemingly similar conditions. The appeal for an unified experimental procedure for the investigation of processes in Fe^0/H_2O systems is reiterated.

1. Introduction

Permeable reactive barriers using elemental iron-based alloys (Fe^0-based alloys widely termed as zerovalent iron) as a reactive medium have been proven to be an efficient and affordable technology for removing inorganics and organics species from groundwater [1–7]. Even living species like viruses have been successfully removed [8]. Despite 15 years of intensive investigations, the removal mechanisms of contaminants in Fe^0 treatment systems are still not well understood [9,10]. In fact, the well-established premise that contaminant removal results from the low electrode potential of the redox couple Fe^{II}/Fe^0 ($E^0 = -0.44$ V) cannot explain why redox-insensitive species are quantitatively removed [11,12]. However, understanding the nature of primary processes yielding to contaminant removal in Fe^0/H_2O systems is of fundamental importance for advancing technological applications. The accurate knowledge of these processes will favour the identification of factors dominating the general reactivity of Fe^0/H_2O systems, which is of fundamental importance for the long-term stability of iron reactive barriers. A more rational devising of Fe^0 treatment systems for an effective and economical contaminant removal could be achieved.

Fe^0 oxidation releases dissolved iron species (Fe^{II}, Fe^{III}) which hydrolyse with increasing pH and precipitate primarily as hydrous oxides (oxide-film) or corrosion products (CP). Oxide-films (CP) of varied composition and thickness develop at all aqueous Fe^0/H_2O interfaces [13,14]. Therefore, an aqueous Fe^0 treatment system (Fe^0/H_2O system) is made up of Fe^0, iron oxides (oxide-film), and water (H_2O). Contaminant adsorption onto the oxide-film and reduction by Fe^0 have mostly been evaluated as separate, independent processes that occur simultaneously or sequentially on metal surfaces. However, contaminants may be primarily quantitatively sequestered by in situ generated hydrous iron oxides (co-precipitation) [11,12]. Initial corrosion products polymerise and precipitate, first as very reactive oxides having short-range crystalline order and after aging as crystalline oxides [15–18]. Subsequent abiotic direct reduction (electrons are transferred from Fe^0) or indirect reduction (electrons from Fe^{II}, H/H_2) of adsorbed or co-precipitated contaminants is possible. As a rule co-precipitation occurs whenever the precipitation of a major species (e.g., iron oxide) takes place in the presence of foreign species (e.g., contaminants) and has been documented for organics [16,17,19,20], inorganics [21–23] and living species [8] under various conditions. Generally, adsorption and co-precipitation are considered to be related such that in order for co-precipitation to occur, sorption to the surface of a forming solid occurs and the adsorbed species is then sequestered in the matrix of the precipitating phase (e.g., iron hydroxide). However, co-precipitation in Fe^0/H_2O systems may be

* Tel.: +49 551 39 3191; fax: +49 551 39 9379.
E-mail address: cnoubac@gwdg.de.

0304-3894/$ – see front matter © 2008 Elsevier B.V. All rights reserved.
doi:10.1016/j.jhazmat.2008.11.001

primarily regarded as a non-specific removal mechanism [11,17] as to be demonstrated in this study of a process involving the discoloration of methylene blue (MB).

Methylene blue is a well-known redox indicator [24] and is a cationic thiazine dye with the chemical name tetramethylthionine chloride. It has a characteristic deep blue colour in the oxidized state; the reduced form (leukomethylene blue (LMB)) is colorless. MB has been widely used in environmental sciences primarily to access the suitability of various materials for wastewater discoloration [25–29]. The mechanism of MB removal by Fe^0-based materials which may be suitable for environmental remediation (cast iron, low alloy steel) has not been yet systematically investigated. Imamura et al. [30] investigated the mechanism of adsorption of methylene blue and its congeners onto stainless steel particles. MB has also been used for corrosion inhibition of mild steel in acid solutions [31].

The literature on "Fe^0 technology" is characterized by the fact that, since the effectiveness of Fe^0 reactive walls to degrade solvents was demonstrated, the feasibility of applying Fe^0 to treat other compounds (or group of compounds) are performed without previous systematic investigations [9]. For example, while presenting the discoloration of MB by a Fe/Cu bimetallic system, Ma et al. [28] referenced several works dealing with dyes in general [32–34]. The authors did not specified whether the referenced works have used MB. Furthermore, their experimental procedure did not include a system with Fe^0 alone to evidence the improvement induced by Cu^0 addition.

Given the diversity of contaminant removal mechanisms in a Fe^0/H_2O system, an approach to elucidate the mechanism of contaminant removal in the system is to characterise the removal process of the contaminant in question by a pure adsorbent (e.g., activated carbon (AC)), and model iron corrosion products (Fe_2O_3, Fe_3O_4) under the same experimental conditions [35]. Here, comparing the evolution of contaminant removal in the systems with pure adsorption (AC, Fe_2O_3, Fe_3O_4) and in the system with Fe^0 will help discussing the removal mechanism. Another approach consists in introducing MnO_2 to delay the availability of corrosion products in the system [36]. MnO_2 readily reacts with Fe^{II} from Fe^0 corrosion products: reductive dissolution of MnO_2 by Fe^{II} [37]. If the process of contaminant removal is coupled with the precipitation of iron, then contaminant removal will be delayed as long as the added amount of MnO_2 consumes Fe^{II} for reductive dissolution as it will be presented later.

The present study is an attempt to elucidate the physicochemical mechanism of MB discoloration in Fe^0/H_2O systems by comparing the kinetics and/or the extent of MB discoloration by Fe^0 and different materials: granular activated carbon (GAC or AC), iron oxides (Fe_2O_3, Fe_3O_4) and manganese dioxide (MnO_2). Non-disturbed (not shaken or shaking at 0 min^{-1}) batch experiments were performed in order to allow formation and transformation of corrosion products at the surface of Fe^0 as it occurs in the nature and in column experiments. The effects of various factors (initial pH value, mixing intensity, particle size, Fe^0 source, Cl^-, HCO_3^-, EDTA) on the extent of MB discoloration are discussed. The results show that MB quantitative discoloration is mostly due to co-precipitation with in situ generated corrosion products. Therefore, MB discoloration occurs within the oxide-film on Fe^0.

2. Background of the experimental methodology

A survey of the electrode potentials of the redox couples relevant for the discussion in this study [$Fe^{II}_{(aq)}/Fe^0$, $Fe^{III}_{(aq)}/Fe^{II}_{(aq)}$, $Fe^{III}_{(s)}/Fe^{II}_{(s)}$, MnO_2/Mn^{2+}, O_2/HO^-, and MB^+/LMB (Eqs. (1)–(6))] suggests that from the available iron species, Fe^0 and $Fe^{II}_{(s)}$ can reduce MB. Eq. (2) is that of the adsorbed Fe^{II} known as structural Fe^{II}. The electrode potential of this redox couple was determined by White and Patterson [38]. The electrode potential of Eqs. (3)–(6) shows that $Fe^{III}_{(aq)}$, dissolved O_2 and MnO_2 may re-oxidize colorless LMB to blue MB^+.

Reaction		E^0 (V)
$Fe^{2+} + 2e^- \Leftrightarrow Fe^0$	(1)	−0.44
$Fe^{3+}_{(s)} + e^- \Leftrightarrow Fe^{2+}_{(s)}$	(2)	−0.36 to −0.65
$MB^+ + 2e^- + H^+ \Leftrightarrow LMB$	(3)	0.01
$Fe^{3+}_{(aq)} + e^- \Leftrightarrow Fe^{2+}_{(aq)}$	(4)	0.77
$O_{2(aq)} + 2H_2O + 4e^- \Leftrightarrow 4OH^-$	(5)	0.81
$MnO_2 + 4H^+ + 2e^- \Leftrightarrow Mn^{2+}_{(aq)} + 2H_2O$	(6)	1.23

Reductive MB discoloration in this study may be the result of either (i) Fe^0 corrosion (oxidation to $Fe^{II}_{(aq)}$) (Eq. (1)) or (ii) oxidation of adsorbed Fe^{II} ($Fe^{II}_{(s)}$ to $Fe^{III}_{(s)}$, Eq. (2)). Additionally, MB adsorption onto in situ generated and aged Fe^0 corrosion products and MB entrapment in the structure of forming corrosion products (co-precipitation) are two further discoloration mechanisms. Therefore, it is difficult to resolve the effect of specific redox reactions on MB discoloration from the effects of other processes. To resolve this problem two additives are added to Fe^0: granular activated carbon (GAC) and manganese dioxide (MnO_2). GAC is a pure adsorbent for MB [25] whereas reductive dissolution of MnO_2 has been reported to decolorize MB [39]. The presentation above shows that MnO_2 should re-oxidise reduced LMB (no discoloration). Therefore, MB discoloration in the presence of MnO_2 could only result from adsorption. On the other hand, MnO_2 is known to be reductively dissolved by Fe^{II} [37,40]. By consuming Fe^{II}, MnO_2 accelerates Fe^0 corrosion, producing more adsorption or co-precipitation agents for MB. Increased adsorption is supported by the fact that iron corrosion products are of higher specific surface area (>40 $m^2\,g^{-1}$) than the used Fe^0 (0.29 $m^2\,g^{-1}$). The reductive dissolution of MnO_2 (Eqs. (7) and (8)) produce further new reactive adsorbents (MnOOH and FeOOH).

$$Fe^{2+}_{(aq)} + MnO_2 + 2H_2O \Rightarrow FeOOH + MnOOH + 2H^+ \quad (7)$$

$$2Fe^{2+}_{(aq)} + MnO_2 + 2H_2O \Rightarrow 2FeOOH + Mn^{2+} + 2H^+ \quad (8)$$

Noubactep et al. [36] have shown that MnO_2 retards the availability of free corrosion products for contaminant co-precipitation.

The used methodology for the investigation of the process of MB discoloration mechanism by Fe^0 consists in following the MB discoloration in the presence of MnO_2 ("Fe^0" and "$Fe^0 + MnO_2$" systems). Thus, the availability of corrosion products for MB co-precipitation in the bulk solution is delayed by the addition of MnO_2. It should be kept in mine that MB discoloration and not MB removal is discussed in this study. For the discussion of MB removal TOC measurements for instance should have been necessary to account for MB reduction to LMB which remains in solution.

3. Materials and methods

3.1. Solutions

The MB molecule has a minimum diameter of approximately 0.9 nm [25,41]. As positively charged ions, MB should readily adsorb onto negatively charged surface. That is at $pH > pH_{pzc}$; pH_{pzc} being the pH at the point of zero charge [42,43]. The used initial concentration was 20 mg L^{-1} (~0.063 mM) MB and it was prepared by diluting a 1000 mg L^{-1} stock solution. All chemicals were analytical grade.

Table 1
Main characteristics, iron content and percent methylene blue (MB) discoloration (P) of tested Fe^0 materials.

Supplier[a]	Supplier denotation	Code	Form	d (μm)	Fe (%)	P (%)
MAZ, mbH	Sorte 69[b]	ZVI0	Fillings	–	93[c]	75 ± 2
G. Maier GmbH	FG 0000/0080	ZVI1	Powder	≤80	92[d]	88 ± 2
G. Maier GmbH	FG 0000/0200	ZVI2	Powder	≤200	92[d]	89 ± 1
G. Maier GmbH	FG 0000/0500	ZVI3	Powder	≤500	92[d]	88 ± 1
G. Maier GmbH	FG 0300/2000	ZVI4	Fillings	200–2000	92[d]	81 ± 4
G. Maier GmbH	FG 1000/3000	ZVI5	Fillings	1000–3000	92[d]	77 ± 4
G. Maier GmbH	FG 0350/1200	ZVI6	Fillings	100–2000	92[d]	88 ± 1
Würth	Hartgussstrahlmittel	ZVI7	Spherical	1200	n.d.[e]	66 ± 1
Hermens	Hartgussgranulat	ZVI8	Flat	1500	n.d.	67 ± 2
G. Maier GmbH	Graugussgranulat	ZVI9	Chips		n.d.	71 ± 7
ISPAT GmbH	Schwammeisen	ZVI10	Spherical	9000	n.d.	72 ± 6
ConnellyGPM	CC-1004	ZVI11	Fillings		>96	76 ± 4
ConnellyGPM	CC-1190	ZVI12	Fillings		>96	75 ± 9
ConnellyGPM	CC-1200	ZVI13	Powder		>96	84 ± 1

MB removal were conducted in triplicates for 36 days under non-disturbed conditions. The material code ("code") are from the author, the given form is as supplied; d (μm) is the diameter of the supplied material and the Fe content is given in % mass.

[a] List of suppliers: MAZ (Metallaufbereitung Zwickau, Co) in Freiberg (Germany); Gotthart Maier Metallpulver GmbH (Rheinfelden, Germany), ISPAT GmbH, Hamburg (Germany), Connelly GPM Inc. (USA).

[b] Scrapped iron material.

[c] Mbudi et al. [52].

[d] Average values from material supplier.

[e] Not determined.

3.2. Solid materials

The main Fe^0 material (ZVI0, Table 1) is a readily available scrapped iron. Its elemental composition was found to be: C: 3.52%; Si: 2.12%; Mn: 0.93%; Cr: 0.66%. The material was fractionated by sieving. The fraction 1.6–2.5 mm was used. The sieved Fe^0 was used without any further pre-treatment. Further 13 commercial Fe^0 samples (ZVI1 through ZVI13) were used in the set of experiments aiming at characterizing the impact of Fe^0 source. The main characteristics of these materials are summarized in Table 1, which is quite typical for a large range of powdered and granular Fe^0 used in laboratory investigations and field works.

The used granular activated carbon (GAC or AC from LS Labor Service GmbH, Griesheim) was crushed and sieved. The particle sized fraction ranging from 0.63 to 1.0 mm was used without further characterization. Granular activated carbon is used as porous adsorbent for MB [25,26].

Powdered commercial Fe_2O_3 (Fluka), Fe_3O_4 (Fisher Scientific) and MnO_2 (Sigma–Aldrich) were purchased and used without any further characterization. Fe_2O_3 and Fe_3O_4 were also used as possible MB adsorbents and are proxies for aged iron corrosion products (Table 2).

Broken manganese nodules (MnO_2) collected from the deep sea with an average particle size of 1.5 mm and elemental composition of Mn: 41.8%; Fe: 2.40%; Si: 2.41%; Ni: 0.74%; Zn: 0.22%; Ca: 1.39%; Cu: 0.36% were used. These manganese nodules originated from the pacific ocean (Guatemala-basin: 06°30 N, 92°54 W and 3670 m deep). The target chemically active component is MnO_2, which occurs naturally mainly as birnessite and todorokite [44]. MnO_2 was mainly used to control the availability of in situ generated oxides from Fe^0 corrosion [36,45]. Reductive dissolution of MnO_2 has been reported to degrade a number of organic pollutants [39,46 and Ref. therein]. Zhu et al. [39] reported the quantitative discoloration of MB by deep sea manganese nodules (pelagite).

3.3. Rationale for choice of test conditions

Materials selected for study were known to be effective for adsorbing MB (GAC), discoloring MB (Fe^0, MnO_2) or delaying the availability of iron corrosion products in Fe^0/H_2O systems (MnO_2). Fe_2O_3 and Fe_3O_4 were used to characterize the reactivity of aged corrosion products. Table 2 summarises the function of the individual materials and gives the material surface coverage in individual reaction vessels. The detailed method for the calculation of the surface coverage (θ) is presented by Jia et al. [47]. The minima of reported specific surface area (SSA) values of the adsorbents were used for the estimation of surface coverage. The Fe^0 SSA was earlier measured by Mbudi et al. [52]. The value 120 $Å^2$ is considered for the molecular cross-sectional area of MB [25]. From Table 2 it can be seen that, apart from Fe^0 ($\theta = 31$), all other materials were present in excess "stoichiometry" ($\theta \leq 0.2$). This means that the available surface of Fe^0 can be covered by up to 31 mono-layers of MB, whereas the other materials should be covered only to one fifth with MB ($\theta = 1$ corresponds to a mono-layer coverage). Therefore, depending on the initial pH value and the affinity of MB for the individual materials (pH_{pzc}) and the kinetics of MB diffusion to the reactive sites (material porosity, mixing intensity), the MB discoloration should be quantitative. A survey of the pH_{pzc} values given in Table 2 suggests that MB adsorption onto all used adsorbents should be favourable because the initial pH was 7.8. At this pH value all surfaces are negatively charged; MB is positively charged. Because the available Fe^0 surface can be covered by up to 31 layers of MB, a progressive MB discoloration in presence of Fe^0 is expected. The tests were performed under mechanically non-disturbed conditions; the effect of the shaking intensity was evaluated in separated experiments. Because diffusion is the main mechanism of MB transport under non-disturbed conditions, long reaction times were experienced to identify the main process of aqueous MB discoloration by Fe^0.

3.4. Discoloration studies

Unless otherwise indicated, batch experiments without shaking were conducted. The batches consisted of 5 g L^{-1} of a reactive material (GAC, Fe^0, Fe_2O_3, Fe_3O_4, MnO_2). In some experiments 5 g L^{-1} Fe^0 was mixed with 0 or 5 g L^{-1} AC and MnO_2, respectively. An equilibration time of about 30 days was selected to allow a MB discoloration efficiency of about 80% in the reference system (ZVI0 alone). The extent of MB discoloration by AC, Fe^0, MnO_2, aged (Fe_2O_3, Fe_3O_4) and in situ generated iron oxides was characterized. For this purpose 0.11 g of Fe^0 and 0 or 0.11 g of the additive were allowed to react in sealed sample tubes containing 22.0 mL of

Table 2
Characteristics, surface coverage and function of the individual reactive materials of this study.

System	pH_{pzc}	SSA ($m^2\ g^{-1}$)	$S_{available}$ (m^2)	Coverage (1)	Function
Fe^0	7.6[a]	0.29	0.032	31.3	MB reductant?
$Fe^0 + MnO_2$	–	–	4.432	0.2	–
MnO_2	2.0–6.0[b]	40	4.4	0.2	Delays CP availability
Fe_2O_3	7.5–8.8[c]	60	6.6	0.2	Mimics aged CP
Fe_3O_4	6.8[d]	40	4.4	0.2	Mimics aged CP
GAC	7.0–8.0[e]	200	22	0.1	MB adsorbent
Fe^0 + GAC	–	(–)	22.032	0.1	–

Apart from Fe^0 the given value of specific surface area (SSA) for are the minima of reported data. Apart from Fe_2O_3 the pH at the point of zero charge (pH_{pzc}) is lower than the initial pH value. Therefore, MB adsorption onto the negatively charged surfaces is favourable. The surface coverage is estimated using the method presented by Jia et al. [47]. The total surface that can be covered by the amount of MB present in 22 mL of a 0.063 mM is $S_{MB} = 0.997\ m^2$.

[a] Ref. [48].
[b] Ref. [39].
[c] Ref. [49].
[d] Ref. [50].
[e] Ref. [51].

a MB solution (20 mg L^{-1}) at laboratory temperature (about 20 °C). The tubes (20 mL graded) were filled to the total volume to reduce the head space in the reaction vessels. Initial pH was ~7.8. After equilibration, up to 5 mL of the supernatant solutions were carefully retrieved (no filtration) for MB measurements. In order to fit the calibration curve for quantitative measurements, the maximal dilution factor was four (4).

Apart from experiments aiming at investigating the impact of mixing intensity and that of the initial pH value, the contact vessels were turned over-head at the beginning of the experiment and allowed to equilibrate in darkness to avoid possible photochemical side reactions. At the end of the equilibration time no attempt was made to homogenize the solutions.

3.5. Analytical methods

MB concentrations were determined by a Cary 50 UV–vis spectrophotometer at a wavelength of 664.5 nm using cuvettes with 1 cm light path. The pH value was measured by combined glass electrodes (WTW Co., Germany). Electrodes were calibrated with five standards following a multi-point calibration protocol [53] in agreement with the current IUPAC recommendation [54].

Each experiment was performed in triplicate and averaged results are presented.

4. Results and discussion

After the determination of the residual MB concentration (C) the corresponding percent MB discoloration was calculated according to the following equation (Eq. (9)):

$$P = \left[1 - \frac{C}{C_0}\right] \times 100\% \quad (9)$$

where C_0 is the initial aqueous MB concentration (about 20 mg L^{-1}), while C gives the MB concentration after the experiment. The operational initial concentration (C_0) for each case was acquired from a triplicate control experiment without additive material (so-called blank). This procedure was to account for experimental errors during dilution of the stock solution (1000 mg L^{-1}), MB adsorption onto the walls of the reaction vessels and all other possible side reaction during the experiments.

4.1. MB discoloration by different agents and discoloration mechanism by Fe^0

Fig. 1 shows the time dependent MB discoloration curve for all the investigated materials. The reference system is a blank experiment as presented above. It can be seen that commercial Fe_2O_3 and MnO_2 did not significantly decolourise MB over the whole duration of the experiments. It is well-known, that poorly crystalline natural MnO_2 are more reactive than land-born and synthetic MnO_2 [39,44]. The decreasing order of discoloration efficiency at the end of the experiment was: $Fe^0 > GAC > Fe_3O_4 > MnO_2$. However, the evolution of the individual systems was very different.

(i) As expected from the surface coverage ($\theta = 31$), Fe^0 presents a progressive MB discoloration over the duration of the experiment. The discoloration mechanism can be the reduction to LMB by Fe^0 and $Fe^{II}_{(s)}$ species, adsorption onto in situ generated corrosion products and/or MB co-precipitation with these new corrosion products.
(ii) Fe_3O_4 (20 g L^{-1}) shows a rapid discoloration kinetic for the first 8 days. The discoloration efficiency then remains constant to approximately 60% through the end of the experiment. This behaviour is typical for non-porous adsorbents. Alternatively available pores may be inaccessible for MB.
(iii) MB discoloration through GAC is insignificant at the start of the experiment (10% after 10 days) and then increases progressively to 75% at the end of the experiment (day 36). This behaviour is typical for porous adsorbents.

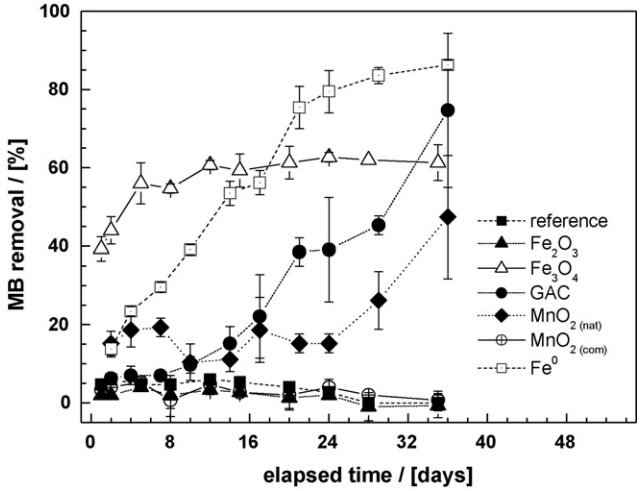

Fig. 1. Methylene blue removal (%) as a function of equilibration time for the six tested reactive materials. The reference system is a blank experiment without additives. Two sets of experiments with MnO_2 were conducted (see the text). The experiments were conducted in triplicate. Error bars give standard deviations. The lines are not fitting functions, they simply connect points to facilitate visualization.

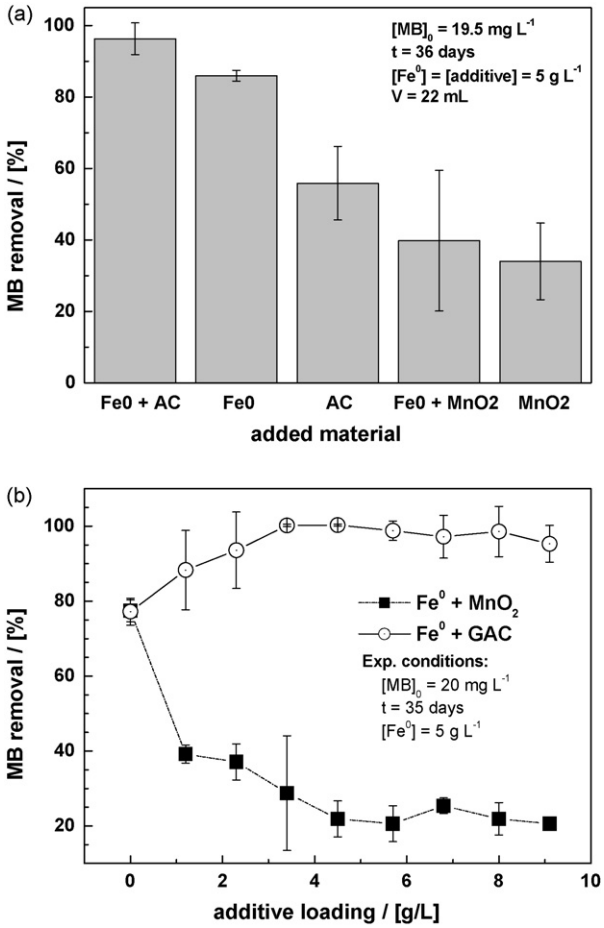

Fig. 2. Methylene blue (MB) discoloration by metallic iron (Fe^0), granular activated carbon (AC), manganese nodule (MnO_2), and the mixtures "Fe^0 + AC" and "$Fe^0 + MnO_2$". (a) Extent of MB discoloration after 36 days, and (b) dependence of the MB discoloration on the additive loading for 35 days. The experiments were conducted in triplicate. Error bars give standard deviations. The lines are given to facilitate visualization.

(iv) $MnO_{2(nat)}$ shows the same behaviour as GAC but the extent of MB discoloration is significantly lower (50% at day 36). Natural MnO_2 acts mostly as adsorbent. MB oxidative discoloration as reported Zhu et al. [39] is not likely to occur under the experimental conditions of this work. Note that, on the contrary to Zhu et al. [39], the experiments in this study were performed under mechanically non-disturbed conditions. While investigating the effect of dynamic conditions, Zhu et al. [39] did not include any non-disturbed system. They just compared shaking ($145\,min^{-1}$) *versus* motor-stirring ($550\,min^{-1}$) and air-bubbling *versus* nitrogen bubbling (both $32\,mL\,s^{-1}$). These mixing conditions are pertinent to wastewater treatment systems but are not reproducible in field-Fe^0 treatment walls, mixing could have favour MB mineralization (oxidation to CO_2) which is an irreversible discoloration.

To better characterize the MB discoloration from aqueous solution by Fe^0, five further experiments have been performed for 36 days with $5\,g\,L^{-1}$ Fe^0 and 0 or $5\,g\,L^{-1}$ of GAC and natural MnO_2.

Fig. 2(a) summarizes the results of MB discoloration in these five systems and Fig. 2(b) depicts the evolution of MB discoloration for $5\,g\,L^{-1}$ Fe^0 and additive (AC or MnO_2) dosages varying from 0 to $9\,g\,L^{-1}$ for an experimental duration of 36 days. Fig. 2(a) shows a regular evolution for the systems involving AC and Fe^0. The MB discoloration efficiency decreases in the order "Fe^0 + AC" > Fe^0 > AC. Considering AC and Fe^0 as pure adsorbents it is expected that the mixture (maximal available binding sites) depicts a larger MB discoloration efficiency than individual materials (Table 2). This trend was not observed for systems involving MnO_2. Here, the decreasing order of MB discoloration efficiency was: Fe^0 > "$Fe^0 + MnO_2$" $\cong MnO_2$. These observations were described by Noubactep et al. [36,45,55] for uranium removal by Fe^0. A "MnO_2 test" was proposed for mechanistic investigations in Fe^0/H_2O systems. The major feature of the "MnO_2 test" is that in reacting with Fe^{II} from Fe^0 oxidation, MnO_2 delays the availability of "free" corrosion products which entrapped contaminants while polymerising and precipitating. "Free" corrosion products are Fe-oxides generated in the vicinity of metallic iron grains. As long as MnO_2 is reductively dissolved, Fe-oxides are generated at its surface or in its vicinity. Thereafter, if co-precipitation is the primary mechanism of contaminant removal, no quantitative removal could occur until enough free corrosion products are available to entrap them while ageing [36]. To confirm this statement the experiment presented in Fig. 2(b) was conducted.

From Fig. 2(b) it can be seen that about $4\,g\,L^{-1}$ activated carbon are sufficient to achieve almost 100% MB discoloration. For [AC] > $4\,g\,L^{-1}$ no additional discoloration was possible. The system with MnO_2 depicts a progressive decrease of MB discoloration with increasing MnO_2 mass loading. The reaction of Fe^{II} species yielding reductive dissolution of MnO_2 is well documented [37,40,56] and yields more adsorbents (e.g., FeOOH, MnOOH—Eqs. (7) and (8)). However, MB discoloration is only quantitative when the oxidative capacity of available MnO_2 for Fe^{II} is exhausted. Thus, MB is removed from the aqueous solution through co-precipitation with in situ generated iron corrosion products. The characterization of the impact of MnO_2 on contaminant removal by Fe^0 occurs ideally under non-disturbed conditions [57]. Note that, if the experiments are performed under (too high) mixing conditions or in columns, increased contaminant removal efficiency in the presence of MnO_2 could have been reported. For example, Burghardt and Kassahun [58] reported increased uranium and radium removal in "$Fe^0 + MnO_2$" systems comparatively to the system with Fe^0 alone. The results of Burghardt and Kassahun [58] are by no means contradictory to those reported here and elsewhere [40] because the net effect of MnO_2 is to promote iron hydroxide formation (or to sustain corrosion) resulting in an increased contaminant removal capacity. Similarly, while Noubactep et al. [36,45,57] reported a delay of U removal by Fe^0 in the presence of pyrite in non-disturbed experiments, Lipczynska-Kochany et al. [59] reported increased carbon tetrachloride degradation in the presence of pyrite. Pyrite is known for its pH lowering capacity, and thus increasing iron corrosion. Non-disturbed experiments allow a better characterization of the progression of involved processes.

4.2. *Effect of Fe^0 source*

Experiments were conducted with 14 different Fe^0 materials: ZVI0 through ZVI13. ZVI1, ZVI2, ZVI3 and ZVI12 were powdered materials. The 10 other samples were granulated materials. The results of MB discoloration are summarised in Table 1. The experimental duration was 35 days. It is shown that powdered materials are more efficient in removing MB than granulated materials (Table 1). The discoloration efficiency for granulated materials varies from 65% for ZVI7 to 80% for ZVI2 (absolute values). That is 15% reactivity difference while the maximum standard deviation for the triplicates in individual experiments was 8.5% (for ZVI12). Therefore, the Fe^0 source (intrinsic reactivity) is a significant operational parameter for laboratory studies. Similar results were reported by Miehr et al. [60] who reported differences in con-

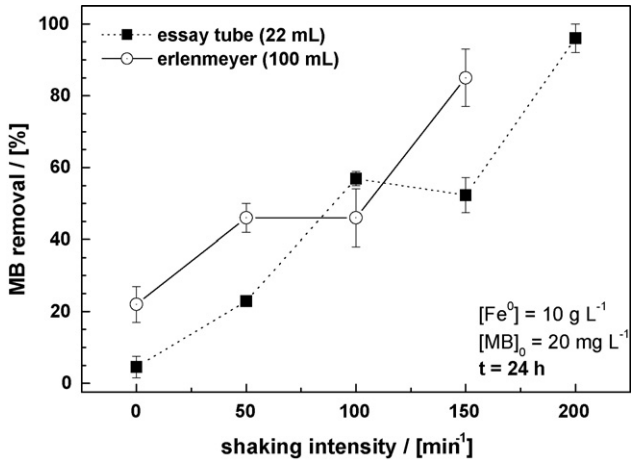

Fig. 3. Effect of the mixing intensity (min^{-1}) on discoloration of MB at initial pH 7.8. The system is mixed on a rotary shaker. The experiments were conducted in triplicate. Error bars give standard deviations. The lines simply connect points to facilitate visualization.

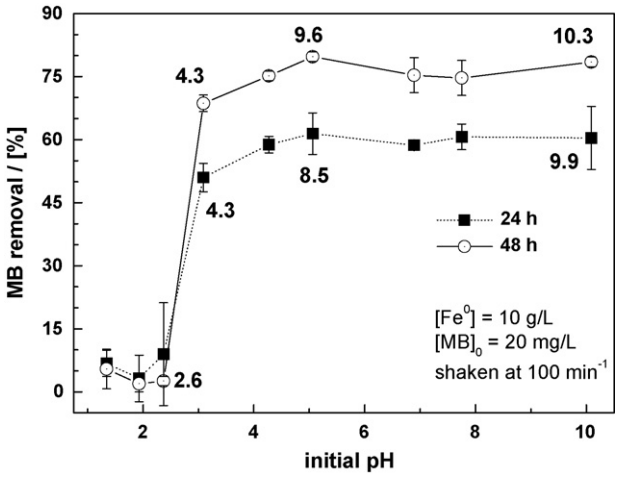

Fig. 4. Effect of initial pH on discoloration of MB by Fe^0 for 24 and 48 h, respectively. The experiments were conducted in triplicate. The reported numbers on the plots are the corresponding final pH values. Error bars give standard deviations. The lines simply connect points to facilitate visualization.

stants of contaminant reduction up to four orders of magnitude when comparing nine types of Fe^0. Therefore, comparing results obtained with different granulated Fe^0 under comparable experimental conditions may lead to erroneous conclusions.

4.3. Effect of shaking intensity

Fig. 3 clearly shows that MB discoloration efficiency increases with the shaking intensity. The experimental duration was 24 h (1 day). The reaction vessels were shaken on a rotary shaker. The MB discoloration rate of 5% at 0 min^{-1} (non-disturbed conditions) increased to 96% at 200 min^{-1}. Between 100 and 150 min^{-1} the MB discoloration rate was constant to 55%. Parallel experiments in 100 mL Erlenmeyer shows comparative results but at 200 min^{-1} the solution was no more limpid and depicted a brown coloration that persisted even after the solutions were allowed to settle for 5 h. Therefore, a mixing intensity of about 150 min^{-1} can be seen as the critical intensity below which MB discoloration studies should be performed. Since applied mixing intensities have not been tested in preliminary works, it is likely that some used mixing operations have been too massive and impractical to mimic subsurface conditions [11]. Mixing intensities as higher as 500 min^{-1} [61,62] have been used to "keep the iron powder suspended".

Generally, Fe^0-based materials show greater contaminant removal efficiency under mixed than under non-disturbed conditions. This removal efficiency is usually attributed to direct reduction whenever the thermodynamics are favourable. However, the open literature on mixed batch experiments demonstrates that a minimum mixing intensity (bubbling, shaking or stirring) is required for complete suspension of solid particles in a liquid medium (e.g., an aqueous solution). Below this critical mixing intensity, the total surface area of the investigated particles is not directly accessible for reaction and the rate of mass transfer depends strongly on stirring rate. Kinetic studies aiming at distinguishing between diffusion-controlled and chemistry-controlled processes have to be conducted at mixing intensities above this critical value [56]. Noubactep [11] has demonstrated that experiments in Fe^0/H_2O systems aiming at investigating processes pertinent to subsurface situations should be conducted below the critical value (mass transfer dependent). For Fe^0, it is obvious, that the value of this critical mixing intensity depends on the particle size (nm, μm, mm). Choe et al. [63] reported a critical value of 40 min^{-1} for nano-scale Fe^0 and performed their experiments at a mixing intensity of 60 min^{-1}. According to the presentation above, Choe et al. [63] would have worked with mixing intensities below 40 min^{-1} to obtain results relevant for groundwater conditions. Furthermore, working at mixing intensities above 40 min^{-1} accelerates iron corrosion yielding more corrosion products which are equally kept suspended in the reaction medium. In the course of corrosion products formation, contaminants are entrapped in the matrix of iron oxides (co-precipitation). It is well know that even low adsorbable species are readily removed from aqueous solutions when precipitation occurs in their presence [16,17,20,21]. As discussed above, MB discoloration mainly occurs through co-precipitation with newly generated corrosion products (see above: "MB discoloration by different agents and discoloration mechanism by Fe^0"). MB discoloration by aged corrosion products was insignificant (Fe_2O_3) or very limited (Fe_3O_4).

4.4. Effect of the initial pH value

The effect of the initial pH on MB discoloration was investigated over the pH range of 1.5–10.0. The initial pH was adjusted by addition of 1.0 M NaOH or HCl. The experiments were conducted under shaken conditions (100 min^{-1}). The pH of the solutions was monitored at the end of the experiments (24 and 48 h). The results are summarised in Fig. 4. MB discoloration was negligible when the final pH was lower than 4 ($P < 10\%$). Once the finial pH exceeded this critical value, MB quantitative discoloration occurred and the extent was pH-independent (60% after 24 h and 76% after 48 h). This observation is consistent with the two main types of aqueous iron corrosion under oxic conditions [64,65]: (i) hydrogen evolution type (pH < 4) and (ii) oxygen absorption type (pH > 4). The characteristic feature of "hydrogen evolution corrosion" is the liberation of hydrogen as hydrogen gas (H_2) at the cathode. Hydrogen evolution corrosion is normally associated with acid electrolytes (e.g., acid mine drainage) and is not relevant for the majority of groundwaters, unless the aquifer is strictly anoxic. The "oxygen absorption" type of immersed Fe^0 corrosion is characteristic of neutral waters. At these pH values (pH > 4.0) iron solubility is low [66]. Thus iron oxide precipitates and MB are removed from the aqueous solution by sequestration (co-precipitation). The results from Fig. 4 validate the concept that all contaminants are primarily adsorbed or/and sequestered by iron corrosion products (co-precipitation)

[11,12]. In fact MB discoloration was quantitative only at final pH > 4, where iron oxides precipitate due to the low solubility of Fe. Within the oxide-film, redox reactions driven by Fe^{II} species have been reported [67]. Therefore, co-precipitated MB can be reduced to LMB but this reaction could not contribute to recorded MB discoloration.

A certain commonly misconception may be found in the literature concerning the process of contaminant removal in Fe^0/H_2O systems due to improper consideration of the two main mechanisms of iron corrosion. Ideally, whenever the initial pH is lower than 4, the pH should be carefully monitored and used to interpret results. From Fig. 4 it can be seen for example, that for an initial pH of 3.0 the final pH was 4.3 and the extent of MB discoloration was slightly lower than that of the experiment with initial pH values ≥ 4 (for the given experimental duration). Consequently, the repeatedly reported lag time for contaminant removal [61,68] is the time to exceed pH 4 (or to enable generation of enough corrosion products for contaminant co-precipitation/sequestration). It must be emphasised that for contaminants (e.g., Cr^{IV}) which are also reducible by aqueous Fe^{II} the extent of their removal at pH < 4 depends on their relative solubility of their reduced form. Regardless from the redox reactivity co-precipitation of contaminant and reaction products occurs at pH > 4. Contaminants, intermediates and final products are possibly entrapped in the matrix of corrosion products.

4.5. Effect of solution chemistry

The effect of solution parameters on MB discoloration by Fe^0 was studied using 0.2 mM of $Al(NO)_3$, $BaCl_2$, $CaCl_2$, $CuCl_2$, EDTA, $(NH_4)_2CO_3$, and $NiCl_2$. Further non-disturbed experiments were performed for 35 days with concentrations of $CaCl_2$, $CuCl_2$ and $NaHCO_3$ varying from 0 to 4 mM (Fig. 5). Fig. 5(a) shows that apart from $(NH_4)_2CO_3$ (90%) all other additives lower the extent of MB discoloration by Fe^0 (78%). The lowest discoloration efficiency (15%) was observed in the presence of EDTA and is consistent with the fact that complexing Fe^{II}/Fe^{III} delays the iron oxide precipitation [69–71] and hence retards MB discoloration. For the four systems containing chloride ions (Cl^-), $NiCl_2$ depicts the lowest MB discoloration efficiency (33%) and $CaCl_2$ the highest (72%). $BaCl_2$ and $CuCl_2$ show very comparable discoloration efficiency (about 60%). This observation is partly consistent with reported results from the literature on corrosion stating that: (i) at low concentration CO_2^{3-} is corrosive, (ii) hardness (Ca^{2+}) is corrosive, while Ni^{2+} has inhibitive properties for iron corrosion. Cu^{2+} would have accelerated Fe^0 corrosion yielding more corrosion products for MB discoloration than in the reference system (Fe^0 alone). Because this was not the case, the experiments reported in Fig. 5(b) were performed.

It can be seen that $NaHCO_3$ enhances MB discoloration for all tested concentrations. The discoloration efficiency increased from 77% at 0.0 mM $NaHCO_3$ to 90% at 0.8 mM $NaHCO_3$ and remains constant for higher $NaHCO_3$ concentrations ($\leq$4 mM). In the experiments with $CaCl_2$ and $CuCl_2$ the initial discoloration rate of 77% first decreases to 70% and 64%, respectively, at an additive concentration of 0.2 mM and subsequently increases to about 74% and remains constant. However, for 4 mM $CuCl_2$ the discoloration efficiency (73% at 2 mM) drops to 30% at 4 mM while the discoloration efficiency in the presence of $CaCl_2$ remains constant (74%). The behaviour of the system with $CuCl_2$ was not further investigated but suggests that if Cu^{2+} is quantitatively produced in a Cu/Fe bimetallic system the reactivity of Fe^0 may be inhibited. This issue is yet to be considered in the Fe^0 technology. Similarly, the comparatively low discoloration efficiency observed in the system with 0.2 mM $NiCl_2$ (33% against 60% for $CaCl_2$) should question the concept of using Ni and Cu as additive metals to form nickel bimetallic systems to "improve the reduction capacity of Fe^0" [28]. No such improvement could be observed in this study (Fig. 5). Discussing the validity of the concept of using bimetallics to improve Fe^0 reactivity is over the scope of this work (see Ref. [72]).

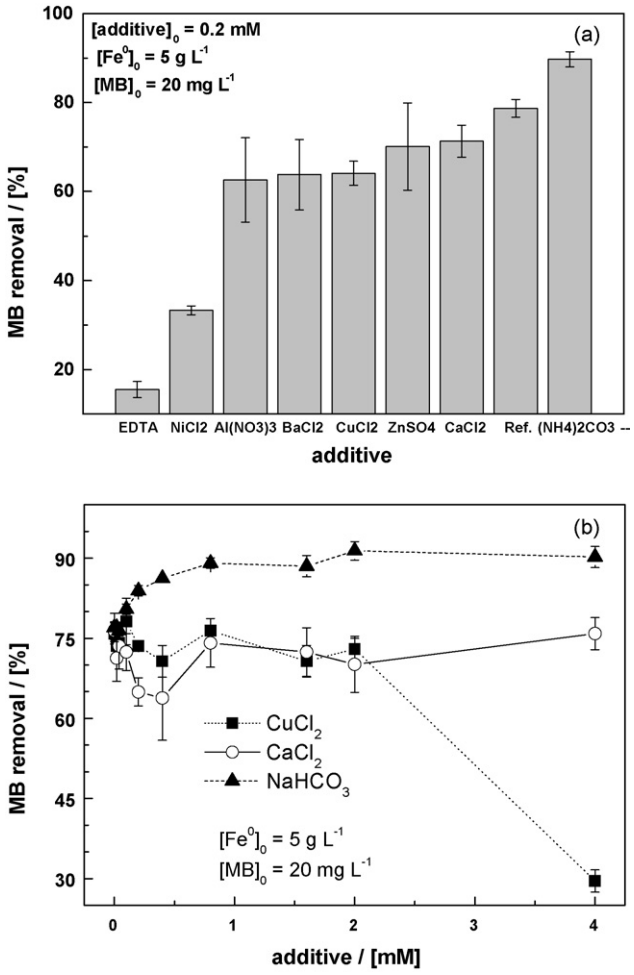

Fig. 5. Effect of solution chemistry on MB discoloration by metallic iron (Fe^0): (a) extent of MB discoloration after 36 days for all tested additives, and (b) dependence of the MB discoloration on selected additive concentrations for 35 days. Ref. in figure "a" refers to the experiment in tap water ("no additive"). The experiments were conducted in triplicate. Error bars give standard deviations. The lines simply connect points to facilitate visualization.

Another important issue from the discussion above is the importance of the cation nature in chloride salts on the extent of MB removal. Generally, chloride ions are known to promote iron corrosion, and therefore increase, sustain or restore Fe^0 reactivity. These observations are mostly attributed to pitting iron corrosion or avoiding the formation of oxide-layers on iron [73,74]. The discussion above demonstrated clearly that the nature of the used salt should be considered in comparing results from independent sources.

5. Conclusions

In summary, despite the low adsorptivity exhibited by MB towards Fe^0, Fe_2O_3 and Fe_3O_4, under the experimental conditions, MB was quantitatively discolored as Fe^0 corrosion proceeded. The extent of MB discoloration was insignificant in experiments in which the availability of in situ generated corrosion products was delayed (MnO_2 addition). Data from the experiments with the systems "Fe^0" and "MnO_2" clearly showed that the kinetics of MB adsorption and reduction by MnO_2 is slower than MB co-

precipitation. Thus, even in systems where direct contaminant reduction (electrons from Fe^0) is likely to occur, co-precipitation will interfere with (or even hamper) mass transport involving Fe^0.

The concept that methylene blue (MB) discoloration from aqueous solution in presence of metallic iron is caused by MB co-precipitation with Fe^0 corrosion products is consistent with many experimental observations, in particular the effects of the initial pH value and the impact of MnO_2 on MB discoloration. Generally, aqueous contaminant removal in Fe^0/H_2O systems can be viewed as a "trickle down" in which a fraction of the targeted contaminant is continuously adsorb onto in situ generated high reactive corrosion products [11]. Contaminants are subsequently entrapped into the structure of ageing corrosion products. In this situation, no observable equilibrium is attained. Therefore, the use of adsorption isotherms (e.g., Freundlich, Langmuir) to interpret data from removal experiments in Fe^0/H_2O systems is not justified (e.g., Ref. [75]). Furthermore, adsorbed or co-precipitated contaminants can be further reduced both by a direct and an indirect mechanism [11,12]. The direct contaminant reduction is only possible when the oxide-film on Fe^0 is electronic conductive or if so-called electron mediators are available [34,76]. Noubactep [11] has clearly shown that the concept of contaminant adsorption and co-precipitation as fundamental removal mechanism is more accurate and considers inherent mistakes of the reductive transformation concept.

It must be concluded that natural Fe^0/H_2O systems consist of core Fe^0 and essentially amorphous Fe oxides that remain to be characterized. In this regard, many investigators have shown the presence of various Fe oxyhydroxides and discussed their role in the process of contaminant removal [77–82]. Strictly, these oxyhydroxides should be considered as transient states as Fe^0/H_2O systems are transforming systems. Therefore, a continuously reacting Fe^0/H_2O system cannot be simply treated being at thermodynamic equilibrium. Thus, characterising the system composition at certain dates is very useful but should be completed by continuously characterizing the system as the contaminants are removed and/or transformed.

With this study, the potential of bulk reactions with selected additives for providing mechanistic information [36] on aqueous contaminant removal is confirmed for the first time using an organic compound. This study also demonstrates the significant impact of selected operational experimental parameters (iron type, shaking intensity, solution chemistry) on the process of MB co-precipitation in Fe^0/H_2O systems. A unified experimental procedure is needed to: (i) avoid further data generation under non-relevant experimental conditions, and (ii) facilitate the inter-laboratory comparison of data. At the term such efforts will provide a confident background for a non-site-specific iron barrier design [83]. Keeping in mine the large spectrum of contaminants that can be removed in Fe^0/H_2O systems and the diversity of Fe^0 materials that are used by individual research groups, it is obvious, that the development of such an unified experimental procedure should be a concerted effort.

Acknowledgments

For providing the iron materials (Fe^0) investigated in this study the author would like to express his gratitude to the branch of the MAZ (Metallaufbereitung Zwickau Co.) in Freiberg (Germany), Gotthart Maier Metallpulver GmbH (Rheinfelden, Germany), Connelly GPM Inc. (USA), Dr. R. Köber from the Institute Earth Science of the University of Kiel and Dr.-Ing. V. Biermann from the Federal Institute for Materials Research and Testing (Berlin, Germany). Mechthild Rittmeier and Emin Özden are acknowledged for technical support. The work was granted by the Deutsche Forschungsgemeinschaft (DFG-No 626/2-2).

References

[1] A.D. Henderson, A.H. Demond, Long-term performance of zero-valent iron permeable reactive barriers: a critical review, Environ. Eng. Sci. 24 (2007) 401–423.
[2] D.F. Laine, I.F. Cheng, The destruction of organic pollutants under mild reaction conditions: a review, Microchem. J. 85 (2007) 183–193.
[3] S.F. O'Hannesin, R.W. Gillham, Long-term performance of an in situ "iron wall" for remediation of VOCs, Ground Water 36 (1998) 164–170.
[4] M.M. Scherer, S. Richter, R.L. Valentine, P.J.J. Alvarez, Chemistry and microbiology of permeable reactive barriers for in situ groundwater clean up, Rev. Environ. Sci. Technol. 30 (2000) 363–411.
[5] P.G. Tratnyek, M.M. Scherer, T.J. Johnson, L.J. Matheson, Permeable reactive barriers of iron and other zero-valent metals, in: M.A. Tarr (Ed.), Chemical Degradation Methods for Wastes and Pollutants: Environmental and Industrial Applications, Marcel Dekker, New York, 2003, pp. 371–421.
[6] N.A. VanStone, R.M. Focht, S.A. Mabury, B.S. Lollar, Effect of iron type on kinetics and carbon isotopic enrichment of chlorinated ethylenes during abiotic reduction on Fe(0), Ground Water 42 (2004) 268–276.
[7] S.D. Warner, D. Sorel, Ten years of permeable reactive barriers: lessons learned and future expectations, in: S.M. Henry, S.D. Warner (Eds.), Chlorinated Solvent and DNAPL Remediation: Innovative Strategies for Subsurface Cleanup, American Chemical Society, Washington, DC, ACS Symp., Ser. 837 (2003), 36–50.
[8] Y. You, J. Han, P.C. Chiu, Y. Jin, Removal and inactivation of waterborne viruses using zerovalent iron, Environ. Sci. Technol. 39 (2005) 9263–9269.
[9] B. Jafarpour, P.T. Imhoff, P.C. Chiu, Quantification and modelling of 2,4-dinitrotoluene reduction with high-purity and cast iron, J. Contam. Hydrol. 76 (2005) 87–107.
[10] J.A. Mielczarski, G.M. Atenas, E. Mielczarski, Role of iron surface oxidation layers in decomposition of azo-dye water pollutants in weak acidic solutions, Appl. Catal. B56 (2005) 289–303.
[11] C. Noubactep, Processes of contaminant removal in "Fe^0–H_2O" systems revisited. The importance of co-precipitation, Open Environ. J. 1 (2007) 9–13.
[12] C. Noubactep, A critical review on the mechanism of contaminant removal in Fe^0–H_2O systems, Environ. Technol. 29 (2008) 909–920.
[13] M. Cohen, The formation and properties of passive films on iron, Can. J. Chem. 37 (1959) 286–291.
[14] K.J. Vetter, General kinetics of passive layers on metals, Electrochim. Acta 16 (1971) 1923–1937.
[15] B. Gu, J. Schmitt, Z. Chen, L. Liang, J.F. McCarthy, Adsorption and desorption of natural organic matter on iron oxide: mechanisms, and models, Environ. Sci. Technol. 28 (1994) 38–46.
[16] Y. Satoh, K. Kikuchi, S. Kinoshita, H. Sasaki, Potential capacity of coprecipitation of dissolved organic carbon (DOC) with iron(III) precipitates, Limnology 7 (2006) 231–235.
[17] U. Schwertmann, F. Wagner, H. Knicker, Ferrihydrite–humic associations magnetic hyperfine interactions, Soil Sci. Soc. Am. J. 69 (2005) 1009–1015.
[18] W.-C. Ying, J.J. Duffy, M.E. Tucker, Removal of humic acid and toxic organic compounds by iron precipitation, Environ. Prog. 7 (1988) 262–269.
[19] E. Tipping, The adsorption of aquatic humic substances by iron oxides, Geochim. Cosmochim. Acta 45 (1981) 191–199.
[20] E. Tipping, Some aspects of the interactions between particulate oxides and aquatic humic substances, Mar. Chem. 18 (1986) 161–169.
[21] R.J. Crawford, I.H. Harding, D.E. Mainwaring, Adsorption and coprecipitation of single heavy metal ions onto the hydrated oxides of iron and chromium, Langmuir 9 (1993) 3050–3056.
[22] H. Füredi-Milhofer, Spontaneous precipitation from electrolytic solutions, Pure Appl. Chem. 53 (1981) 2041–2055.
[23] I. Nirdosh, S.V. Muthuswami, M.H.I. Baird, Radium in uranium mill tailings—some observations on retention and removal, Hydrometallurgy 12 (1984) 151–176.
[24] B.D. Jones, J.D. Ingle, Evaluation of redox indicators for determining sulfate-reducing and dechlorinating conditions, Water Res. 39 (2005) 4343–4354.
[25] A.A. Attia, B.S. Girgis, N.A. Fathy, Removal of methylene blue by carbons derived from peach stones by H_3PO_4 activation: batch and column studies, Dyes Pigments 76 (2008) 282–289.
[26] J. Avom, J.B. Ketcha, C. Noubactep, P. Germain, Adsorption of methylene blue from an aqueous solution onto activated carbons from palm-tree cobs, Carbon 35 (1997) 365–369.
[27] K. Dutta, S. Mukhopadhyay, S. Bhattacharjee, B. Chaudhuri, Chemical oxidation of methylene blue using a Fenton-like reaction, J. Hazard. Mater. 84 (2001) 57–71.
[28] L.M. Ma, Z.G. Ding, T.Y. Gao, R.F. Zhou, W.Y. Xu, J. Liu, Discoloration of methylene blue and wastewater from a plant by a Fe/Cu bimetallic system, Chemosphere 55 (2004) 1207–1212.
[29] S. Pande, S.K. Ghosh, S. Nath, S. Praharaj, S. Jana, S. Panigrahi, S. Basu, T. Pal, Reduction of methylene blue by thiocyanate: kinetic and thermodynamic aspects, J. Colloid Interf. Sci. 299 (2006) 421–427.
[30] K. Imamura, E. Ikeda, T. Nagayasu, T. Sakiyama, K. Nakanishi, Adsorption behavior of methylene blue and its congeners on a stainless steel surface, J. Colloid Interf. Sci. 245 (2002) 50–57.
[31] E.E. Oguzie, Corrosion inhibition of mild steel in hydrochloric acid solution by methylene blue dye, Mater. Lett. 59 (2005) 1076–1079.
[32] J. Cao, L. Wei, Q. Huang, L. Wang, S. Han, Reducing degradation of azo dye by zero-valent iron in aqueous solution, Chemosphere 38 (1999) 565–571.

[33] S. Nam, P.G. Tratnyek, Reduction of azo dyes with zero-valent iron, Water Res. 34 (2000) 1837–1845.
[34] E.J. Weber, Iron-mediated reductive transformations: investigation of reaction mechanism, Environ. Sci. Technol. 30 (1996) 716–719.
[35] F. dos Santos Coelho, J.D. Ardisson, F.C.C. Moura, R.M. Lago, E. Murad, J.D. Fabris, Potential application of highly reactive Fe(0)/Fe_3O_4 composites for the reduction of Cr(VI) environmental contaminants, Chemosphere 71 (2008) 90–96.
[36] C. Noubactep, G. Meinrath, J.B. Merkel, Investigating the mechanism of uranium removal by zerovalent iron materials, Environ. Chem. 2 (2005) 235–242.
[37] D. Postma, C.A.J. Appelo, Reduction of Mn-oxides by ferrous iron in a flow system: column experiment and reactive transport modelling, Geochim. Cosmochim. Acta 64 (2000) 1237–1247.
[38] A.F. White, M.L. Paterson, Reduction of aqueous transition metal species on the surface of Fe(II)-containing oxides, Geochim. Cosmochim. Acta 60 (1996) 3799–3814.
[39] M.-X. Zhu, Z. Wang, L.-Y. Zhou, Oxidative decolorization of methylene blue using pelagite, J. Hazard. Mater. 150 (2008) 37–45.
[40] D.F.A. Koch, Kinetics of the reaction between manganese dioxide and ferrous ion, Aust. J. Chem. 10 (1957) 150–159.
[41] H. Valdes, M. Sanchez-Polo, J. Rivera-Utrilla, C.A. Zaror, Effect of ozone treatment on surface properties of activated carbon, Langmuir 18 (2002) 2111–2116.
[42] V. Ender, On the structure of the metal-oxide/H_20 interface - formation of potentials and equilibrium of charge, Acta Hydrochim. Hydrobiol. 19 (1991) 199–208.
[43] M.R. Hoffmann, S.T. Martin, W. Choi, D.W. Bahnemann, Environmental applications of semiconductor photocatalysis, Chem. Rev. 95 (1995) 69–96.
[44] J.E. Post, Manganese oxide minerals: crystal structures and economic and environmental significance, Proc. Natl. Acad. Sci. U.S.A. 96 (1999) 3447–3454.
[45] C. Noubactep, A. Schöner, G. Meinrath, Mechanism of uranium (VI) fixation by elemental iron, J. Hazard. Mater. 132 (2006) 202–212.
[46] H. Zhang, C.-H. Huang, Oxidative transformation of triclosan and chlorophene by manganese oxides, Environ. Sci. Technol. 37 (2003) 2421–2430.
[47] Y. Jia, P. Aagaard, G.D. Breedveld, Sorption of triazoles to soil and iron minerals, Chemosphere 67 (2007) 250–258.
[48] T. Liu, D.C.W. Tsang, I.M.C. Lo, Chromium(VI) reduction kinetics by zero-valent iron in moderately hard water with humic acid: iron dissolution and humic acid adsorption, Environ. Sci. Technol. 42 (2008) 2092–2098.
[49] K. Hanna, Adsorption of aromatic carboxylate compounds on the surface of synthesized iron oxide-coated sands, Appl. Geochem. 22 (2007) 2045–2053.
[50] S. Yean, L. Cong, C.T. Yavuz, J.T. Mayo, W.W. Yu, A.T. Kan, V.L. Colvin, M.B. Tomson, Effect of magnetite particle size on adsorption and desorption of arsenite and arsenate, J. Mater. Res. 20 (2005) 3255–3264.
[51] M.I. Bautista-Toledo, J.D. Méndez-Díaz, M. Sánchez-Polo, J. Rivera-Utrilla, M.A. Ferro-García, Adsorption of sodium dodecylbenzenesulfonate on activated carbons: effects of solution chemistry and presence of bacteria, J. Colloid Interf. Sci. 317 (2008) 11–17.
[52] C. Mbudi, P. Behra, B. Merkel, The effect of background electrolyte chemistry on uranium fixation on scrap metallic iron in the presence of arsenic, Paper Presented at the Inter. Conf. Water Pollut. Natural Porous Media (WAPO2), Barcelona (Spain), April 11–13 (2007), 8 p.
[53] G. Meinrath, P. Spitzer, Uncertainties in determination of pH, Mikrochem. Acta 135 (2000) 155–168.
[54] R.P. Buck, S. Rondinini, A.K. Covington, F.G.K. Baucke, C.M.A. Brett, M.F. Camoes, M.J.T. Milton, T. Mussini, R. Naumann, K.W. Pratt, P. Spitzer, G.S. Wilson, Measurement of pH. Definition, standards, and procedures (IUPAC Recommendations 2002), Pure Appl. Chem. 74 (2002) 2169–2200.
[55] C. Noubactep, G. Meinrath, P. Dietrich, B. Merkel, Mitigating uranium in ground water: prospects and limitations, Environ. Sci. Technol. 37 (2003) 4304–4308.
[56] T. Tekin, M. Bayramoglu, Kinetics of the reduction of MnO_2 with Fe^{2+} ions in acidic solutions, Hydrometallurgy 32 (1993) 9–20.
[57] C. Noubactep, Investigations for the passive in-situ Immobilization of uranium (VI) from water (in German), Dissertation, TU Bergakademie Freiberg, Wiss. Mitt. Institut für Geologie der TU Bergakademie Freiberg, Band, 21 (2003) 140, ISSN1433-1284.
[58] D. Burghardt, A. Kassahun, Development of a reactive zone technology for simultaneous in situ immobilisation of radium and uranium, Environ. Geol. 49 (2005) 314–320.
[59] E. Lipczynska-Kochany, S. Harms, R. Milburn, G. Sprah, N. Nadarajah, Degradation of carbon tetrachloride in the presence of iron and sulphur containing compounds, Chemosphere 29 (1994) 1477–1489.
[60] R. Miehr, P.G. Tratnyek, Z.J. Bandstra, M.M. Scherer, J.M. Alowitz, J.E. Bylaska, Diversity of contaminant reduction reactions by zerovalent iron: role of the reductate, Environ. Sci. Technol. 38 (2004) 139–147.
[61] Z. Hao, X. Xu, D. Wang, Reductive denitrification of nitrate by scrap iron filings, J. Zhejiang Univ. Sci. 6B (2005) 182–187.
[62] W.S. Pereira, R.S. Freire, Azo dye degradation by recycled waste zero-valent iron powder, J. Braz. Chem. Soc. 17 (2006) 832–838.
[63] S. Choe, Y.Y. Chang, K.Y. Hwang, J. Khim, Kinetics of reductive denitrification by nanoscale zero-valent iron, Chemosphere 41 (2000) 1307–1311.
[64] G.W. Whitman, R.P. Russel, V.J. Altieri, Effect of hydrogen-ion concentration on the submerged corrosion of steel, Ind. Eng. Chem. 16 (1924) 665–670.
[65] E.R. Wilson, The Mechanism of the corrosion of iron and steel in natural waters and the calculation of specific rates of corrosion, Ind. Eng. Chem. 15 (1923) 127–133.
[66] D. Rickard, The solubility of FeS, Geochim. Cosmochim. Acta 70 (2006) 5779–5789.
[67] M. Stratmann, J. Müller, The mechanism of the oxygen reduction on rust-covered metal substrates, Corros. Sci. 36 (1994) 327–359.
[68] C.G. Schreier, M. Reinhard, Transformation of chlorinated organic compounds by iron and manganese powders in buffered water and in landfill leachate, Chemosphere 29 (1994) 1743–1753.
[69] L.J. Matheson, P.G. Tratnyek, Reductive dehalogenation of chlorinated methanes by iron metal, Environ. Sci. Technol. 28 (1994) 2045–2053.
[70] C. Noubactep, G. Meinrath, P. Dietrich, M. Sauter, B. Merkel, Testing the suitability of zerovalent iron materials for reactive walls, Environ. Chem. 2 (2005) 71–76.
[71] E.M. Pierce, D.M. Wellman, A.M. Lodge, E.A. Rodriguez, Experimental determination of the dissolution kinetics of zero-valent iron in the presence of organic complexants, Environ. Chem. 4 (2007) 260–270.
[72] C. Noubactep, On the operating mode of bimetallic systems for environmental remediation. J. Hazard. Mater. (in press) available online 13 August 2008, doi:10.1016/j.jhazmat.2008.08.004.
[73] R. Hernandez, M. Zappi, C.-H. Kuo, Chloride effect on TNT degradation by zerovalent iron or zinc during water treatment, Environ. Sci. Technol. 38 (2004) 5157–5163.
[74] J.S. Kim, P.J. Shea, J.E. Yang, J.-E. Kim, Halide salts accelerate degradation of high explosives by zerovalent iron, Environ. Pollut. 147 (2007) 634–641.
[75] D.R. Burris, T.J. Campbell, V.S. Manoranjan, Sorption of trichloroethylene and tetrachloroethylene in a batch reactive metallic iron-water system, Environ. Sci. Technol. 29 (1995) 2850–2855.
[76] P.G. Tratnyek, M.M. Scherer, B. Deng, S. Hu, Effects of natural organic matter, anthropogenic surfactants, and model quinones on the reduction of contaminants by zero-valent iron, Water Res. 35 (2001) 4435–4443.
[77] P.D. Mackenzie, D.P. Horney, T.M. Sivavec, Mineral precipitation and porosity losses in granular iron columns, J. Hazard. Mater. 68 (1999) 1–17.
[78] J.A. Mielczarski, G.M. Atenas, E. Mielczarski, Role of iron surface oxidation layers in decomposition of azo-dye water pollutants in weak acidic solutions, Appl. Catal. B: Environ. 56 (2005) 289–303.
[79] D.H. Phillips, B. Gu, D.B. Watson, Y. Roh, L. Liang, S.Y. Lee, Performance evaluation of a zerovalent iron reactive barrier: mineralogical characteristics, Environ. Sci. Technol. 34 (2000) 4169–4176.
[80] K. Ritter, M.S. Odziemkowski, R.W. Gillham, An in situ study of the role of surface films on granular iron in the permeable iron wall technology, J. Contam. Hydrol. 55 (2002) 87–111.
[81] M.M. Scherer, B.A. Balko, P.G. Tratnyek, The role of oxides in reduction reactions at the metal-water interface, in: D. Sparks, T. Grundl (Eds.), Kinetics and Mechanism of Reactions at the Mineral/Water Interface, American Chemical Society, Washington, DC, 1999, pp. 301–322.
[82] M.M. Scherer, K. Johnson, J.C. Westall, P.G. Tratnyek, Mass transport effects on the kinetics of nitrobenzene reduction by iron metal, Environ. Sci. Technol. 35 (2001) 2804–2811.
[83] K.L. McGeough, R.M. Kalin, P. Myles, Carbon disulfide removal by zero valent iron, Environ. Sci. Technol. 41 (2007) 4607–4612.